Food Hydrocolloids 105 (2020) 105805

Contents lists available at ScienceDirect

Food Hydrocolloids

journal homepage: http://www.elsevier.com/locate/foodhyd

Amylose crystal seeds: Preparation and their effect on starch retrogradation

Bihua Zhu [a,b], Jinling Zhan [a,c], Long Chen [a,b], Yaoqi Tian [a,b,*]

[a] State Key Laboratory of Food Science and Technology, Jiangnan University, 1800 Lihu Road, Wuxi, 214122, China
[b] School of Food Science and Technology, Jiangnan University, 1800 Lihu Road, Wuxi, 214122, China
[c] National Engineering Laboratory for Cereal Fermentation Technology, Jiangnan University, Wuxi, 214122, China

ARTICLE INFO

Keywords:
Amylose crystal seeds
Long-term retrogradation
X-ray diffraction
Fourier transform infrared spectroscopy
Differential scanning calorimetry

ABSTRACT

The relationship between the short-term retrogradation dominated by amylose and the long-term retrogradation dominated by amylopectin still lacks specific experimental confirmation. In order to explore this relationship, four types of amylose crystal seeds (ACS) were prepared and added to native rice starch to intervene the long-term retrogradation. The average particle size of ACS was 200–450 nm. The maximum relative crystallinity of retrograded starch increased from 13.64% to 17.88% under the intervention of ACS. The ratio of absorbance at 1047 to 1022 cm^{-1} of retrograded starch increased from 0.670 to the maximum 0.887. The retrogradation rate constant increased significantly from 0.024 up to 0.051 d^{-1}. The long-range order, short-range order, and retrogradation rate of retrograded starch all increased significantly, which indicated that the intervention of ACS promoted the long-term retrogradation of starch. These findings provided data support for the analysis of correlation between different stages of starch retrogradation.

1. Introduction

Starch retrogradation is a process, which occurs when the molecular motion of starch paste slows down due to a decrease in temperature. During the process of retrogradation, amylose and amylopectin rearrange into microcrystalline forms through the formation of hydrogen bonds to yield a more ordered or crystalline state (Fu, Wang, Li, Zhou, & Adhikari, 2013; Karim, Norziah, & Seow, 2000). Starch retrogradation includes two stages: short-term retrogradation and long-term retrogradation (Funami et al., 2009; Ronda & Roos, 2008). In the short-term retrogradation stage, it is mainly the formation and accumulation of double helix structure of amylose, and in the long-term retrogradation stage, it is mainly the formation of double helix structure between amylopectin outer branches and the ordered accumulation between double helixes (Chen, Ren, Zhang, Tong, & Rashed, 2015). The retrogradation rate in short-term retrogradation dominated by amylose is fast, and the retrogradation rate in long-term retrogradation dominated by amylopectin is slow (Imberty, Bulecon, Tran, & Péerze, 1991; Swinkels, 1985). Besides, Tukomane et al. (2008) found that the content of amylose in rice starch was closely related to its retrogradation degree, and the higher amylose content was, the more easily starch retrograded. Consequently, it is generally recognized in theory that short-term retrogradation provides the crystal seed for long-term retrogradation. But due to the complexity of retrogradation and limited research methods of further analyzing the structure of crystal cells, there are no specific data to support this hypothesis up to now. Furthermore, the relationship between short-term retrogradation and long-term retrogradation provides the basis for the preparation of starch-based products with slow digestion times and the development of anti-retrogradation technology for rice noodle products. According to the classical kinetics model of polymer crystallization, crystallization includes nucleation, growth, and the formation of a perfect crystal (Marentette & Brown, 1993). This also holds true in the case of starch recrystallization (Bulkin, Kwak, & Dea, 1987). In the starch retrogradation system, the essence of retrogradation is also nucleation and crystal growth, with the crystal nucleus promoting growth and perfection. However, in practice, the processes of nucleation and growth during retrogradation are difficult to separate in the starch retrogradation system.

Based on this, an innovative research idea was put forward. As mentioned before, the gel structure observed during short-term retrogradation is mainly formed via amylose rearrangement into an ordered structure. Therefore, in this study, short-term retrograded rice amylose was selected as a crystal seed to simulate the short-term retrogradation of starch and it was added to the starch recrystallization to study its impact on the long-term retrogradation. Amylose crystal seeds (ACS) were prepared by acid hydrolysis of short-term retrograded rice amylose

* Corresponding author. State Key Laboratory of Food Science and Technology, Jiangnan University, 1800 Lihu Road, Wuxi, 214122, China.
E-mail address: yqtian@jiangnan.edu.cn (Y. Tian).

https://doi.org/10.1016/j.foodhyd.2020.105805
Received 9 October 2019; Received in revised form 31 January 2020; Accepted 24 February 2020
Available online 25 February 2020
0268-005X/

Table 1
The average cooling rates of gelatinized rice amylose which cooled at different ambient temperatures.

Sample name	Ambient temperature (°C)	Average cooling rate (°C/min)
RA-80	−80	6.71 ± 0.15[a]
RA-18	−18	3.00 ± 0.12[b]
RA4	4	1.78 ± 0.09[c]
RA25	25	0.75 ± 0.13[d]

RA-80, the gelatinized rice amylose cooled at −80 °C; RA-18, the gelatinized rice amylose cooled at −18 °C; RA4, the gelatinized rice amylose cooled at 4 °C; and RA25, the gelatinized rice amylose cooled at 25 °C.
Values in the same column with different lowercase letters are significantly different ($p < 0.05$).

and added into the paste of native rice starch to investigate the long-term retrogradation process.

2. Materials and methods

2.1. Materials

Native rice starch was purchased from Jinnong Development Co., Ltd. (Jiangxi, China) with an amylose content of 12.2%. All reagents, such as n-butyl alcohol, isoamyl alcohol, sodium hydroxide, sulfuric acid, potassium chloride, and potassium bromide were of analytical purity (China Pharmaceutical Group Co., Ltd., China). Rice amylose was extracted according to the method of Cheng, Xu, Xiong, and Zhao (2008).

2.2. Preparation of ACS

Rice amylose (40 g) was dispersed into deionized water (200 mL) to make a final concentration of 20% (w/v). The starch suspension was pregelatinized in boiling water for 30 min, then heated at 121 °C for 20 min in a high-pressure steam sterilization pot. The starch paste was cooled at different rates. The specific cooling conditions are shown in Table 1. The rice amylose pastes cooled at −80, −18, 4, and 25 °C were named as RA-80, RA-18, RA4, and RA25, respectively. All samples were placed in biochemical incubator (LRH-500F, Yiheng Scientific Instrument Co., Ltd, China) to be kept at 25 °C once the temperature decreased to 25 °C. The whole short-term retrogradation process lasted for 12 h. The cold paste was dried, ground, and screened over 100 meshes. Up to this step, the preparation of ACS had been preliminarily completed but it still contained a considerable part of amorphous area, which might have impact on later experiment. The methods to remove the amorphous area of starch included acid hydrolysis and amylase hydrolysis (Lian, Liu, Guo, Li, & Wu, 2013).

In this experiment, the amylose crystal seeds were prepared by acid hydrolysis following Angellier's method (2004) to remove amorphous area. Acid hydrolysis removes amorphous regions of short-term retrograded starch, improving the relative crystallinity of ACS. Briefly, the retrograded starch was hydrolyzed with 3.16 mol/L sulfuric acid at 45 °C for 7 days. Once sulfuric acid hydrolysis was completed, samples were washed to neutrality with deionized water. Starch nanocrystals had small particle size and many atoms on its surface which possess high activity. Due to the lack of coordination of surface atoms, they tended to combine with other atoms driven by high surface energy to keep stable, resulting in the occurrence of agglomeration. ACS readily agglomerated after drying and their average size was around 4.4 μm (Angellier, Choisnard, Molina-Boisseau, Ozil, & Dufresne, 2004). Putting the starch nanocrystals into suspension could alleviate the agglomeration, so amylose crystal seeds were stored in suspension for later use.

2.3. Preparation of retrograded starch

Native rice starch was added to distilled water to obtain a final starch suspension of 10% (w/v) and gelatinized in boiling water for 30 min. When the temperature of the non-control groups dropped to 60 °C, ACS were added to the starch paste and the starch-ACS mixtures were stirred. All samples were stored at 4 °C and were taken out on day 0, 1, 3, 5, 7, 14, and 21. Finally, the starch gel was dried, ground, screened, and packed in self-sealing bags for further use.

2.4. Characterization of samples

2.4.1. Dynamic light scattering (DLS)

The suspension of ACS was diluted to 0.1‰ (w/v), and subjected to sonication for 10 min to break the agglomerated particles. Upon finishing it, the suspension was transferred to the sample cell of zeta potential instrument (Nano Brook Omni, Bookhaven Inc., USA) immediately. Measurement was taken under DLS model at 25 °C.

2.4.2. X-ray diffraction analysis (XRD)

All samples were placed in a sealed dryer and equilibrated with a saturated potassium chloride solution for 24 h. After that, the crystalline structures of the powders were characterized using an X-ray diffractometer (D2 PHASER, Bruker AXS Inc., Germany) with 40 kV voltage and 30 mA Cu-Ka radiations. The X-ray diffractometer scanned from 4° to 40° (2θ) at a rate of 5.75°/min. The relative crystallinity was calculated according to eq. (1) (Chen et al., 2018):

$$R_c = \frac{A_C}{A_c + A_a} \times 100\% \quad (1)$$

R_c means the relative crystallinity of the sample, while A_a and A_c mean the areas of amorphous region and crystalline region, respectively. A_a and A_c are calculated by Jade 6.5 software (Materials Data Inc., Livermore, CA, USA).

The XRD diagram of the starch sample was imported into the Jade 6.5 software for fitting. The intensity data obtained from theoretical calculation was fitted to the experimental intensity with a certain peak shape function. The values of peak function and structural parameters were adjusted continuously in the process of fitting to make the calculated strength gradually close to the experimental strength value. The fitting method was the least square method. When the difference M between the two strength values was the smallest, the fitting was completed. M was calculated as follows:

$$M = \sum W_i (Y_{ai} - Y_{ci})^2 \quad (2)$$

W_i means scale factor, Y_{ai} and Y_{ci} correspond to actual intensity and calculation intensity of step i of step-scan, respectively.

The fitting results were then refined with R value as the index. Results were usable when R < 9%.

R was calculated as follows:

$$R = \frac{\sum |Y_{io} - Y_{ic}|}{\sum Y_{io}} \quad (3)$$

Y_{io} is the intensity measurement at the i-th count point, Y_{ic} is the intensity calculation at the i-th count point.

2.4.3. Fourier transform infrared spectroscopy (FTIR)

The starch powder and potassium bromide were mixed in a mass ratio of 1:20 and ground by agate mortar and pestle. The IR spectra were measured using FTIR (Is10, Nicolet Inc., America). The scanning wavenumber range was 4000–400 cm^{-1}, the resolution ratio was 4 cm^{-1}, and the scanning times was 16. A pure potassium bromide tablet was used as blank.

The full FTIR spectra were baseline-corrected automatically by using OMNIC 8.0 before the spectra between 1100 and 950 cm^{-1} were deconvoluted with a half-band width of 31 cm^{-1} and an enhancement factor of 2.1. Then the absorbance ratio at 1047 and 1022 cm^{-1}, 1022 and 995 cm^{-1} after deconvolution were used to measure the short-range

Table 2
The thermal parameters of native rice starch and four types of amylose crystal seeds.

Samples	T_o (°C)	T_p (°C)	T_c (°C)	ΔH (mJ/mg)
ACS-80	79.56 ± 0.41^c	87.15 ± 0.19^b	93.68 ± 0.43^c	0.15 ± 0.02^c
ACS-18	83.67 ± 0.22^b	91.85 ± 0.30^a	98.38 ± 0.31^{ab}	0.22 ± 0.04^c
ACS4	84.70 ± 0.16^a	92.49 ± 0.24^a	99.22 ± 0.35^a	0.44 ± 0.05^b
ACS25	84.35 ± 0.25^a	91.47 ± 0.22^a	98.11 ± 0.84^b	0.36 ± 0.02^b

ACS-80, amylose crystal seeds prepared by RA-80; ACS-18, amylose crystal seeds prepared by RA-18; ACS4, amylose crystal seeds prepared by RA4; and ACS25, amylose crystal seeds prepared by RA25.
Values in the same column with different lowercase letters are significantly different ($p < 0.05$).

order of starch.

2.4.4. Differential scanning calorimetry (DSC)

The thermal properties of samples were measured by DSC (SII Nano Technology Inc., Japan) over a temperature range of 20–100 °C and a heating rate of 10 °C/min. The flow rate of N_2 was 20 mL/min. The ratio of sample mass (on a dry basis) to the mass of deionized water was 1:2. The starch suspension was sealed in the aluminum crucible during the measurement, while the empty aluminum crucible was used as a blank. The onset temperature (T_o), peak temperature (T_p), and conclusion temperature (T_c) of different samples were recorded and the enthalpy change (ΔH_i) was calculated. ΔH_i can be used to assess the extent of retrogradation. During storage at 4 °C, changes in enthalpy were analyzed using the Avrami equation which is widely used in studying the isothermal crystallization of starch (Avrami, 1939; Mciver, Axford, Colwell, & Elton, 1968; Yao, Zhang, & Ding, 2002):

$$X_{(t)} = \frac{\Delta H_t - \Delta H_0}{\Delta H_\infty - \Delta H_0} \quad (4)$$

$$1 - X_{(t)} = 1 - \frac{\Delta H_t - \Delta H_0}{\Delta H_\infty - \Delta H_0} = e^{-kt^n} \quad (5)$$

$$\ln[-\ln(1 - X_{(t)})] = \ln k + n \ln t \quad (6)$$

where ΔH_∞ (mJ/mg), ΔH_0 (mJ/mg), and ΔH_t (mJ/mg) mean retrogradation enthalpies at 21, 0, and t days, respectively, n represents the Avrami index, t is the retrogradation time in days, and k is the retrogradation rate constant. The above experiments were repeated at least three times and dynamic parameters of retrogradation were calculated from the Avrami equation.

2.5. Statistical analysis

The data were presented as the mean ± standard deviation. One-way ANOVA with Duncan's test using SPSS 20.0 (SPSS Inc., Chicago, USA) was applied to evaluate the statistical significance and standard deviation of the data. Throughout the study, $p < 0.05$ was considered to be statistically significant.

3. Results and discussion

3.1. Characterization of ACS

3.1.1. Thermal stability of ACS

As shown in Table 2, all ACS had endothermic peaks above 79 °C. Therefore, ACS that was added, as described in section 2.3, was not destroyed because the temperature of the starch paste was 60 °C, lower than the fusion temperature of ACS.

3.1.2. Average particle size of ACS

The particle size data of ACS obtained by DLS are shown in Table 3. The average particle size of ACS-80, ACS-18, ACS4 and ACS25 were 438.61 nm, 303.78 nm, 246.42 nm, and 279.43 nm, respectively. Rice starch particles with a size range of 2–10 μm were the smallest in known grains and owned irregular polygon shape (BeMiller & Whistler, 2008). In the process of gelatinization, starch molecular chains swelled and became irregular lumps. The ACS with nano size added before retrogradation could enter the inner part of gelatinized starch and contact with starch chains successfully, so it could play a role of induction.

Table 3
Average particle size of ACS.

Sample name	ACS-80	ACS-18	ACS4	ACS25
Average particle size (nm)	438.61 ± 3.57^a	303.78 ± 4.23^b	246.42 ± 3.02^d	279.43 ± 2.68^c

ACS-80, amylose crystal seeds prepared by RA-80; ACS-18, amylose crystal seeds prepared by RA-18; ACS4, amylose crystal seeds prepared by RA4; and ACS25, amylose crystal seeds prepared by RA25.
Values in the same line with different lowercase letters are significantly different ($p < 0.05$).

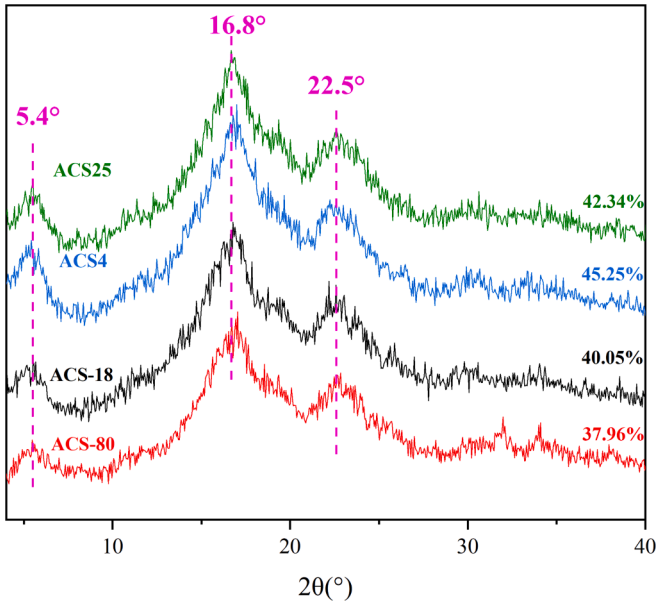

Fig. 1. X-ray diffraction patterns and relative crystallinity of four types of ACS (ACS-80, ACS-18, ACS4 and ACS25, respectively, from bottom to up; and 2θ means the diffraction angle).

3.1.3. Crystal structure of ACS

The X-ray diffraction patterns and the relative crystallinity of ACS are shown in Fig. 1. All four types of ACS exhibited typical B-type diffraction patterns with peaks at 2θ approximately 5.4°, 16.8°, and 22.5° (Kim, Kim, & Shin, 1997). This result was consistent with previous findings. When the moisture content of the starch paste was lower than 19% during retrogradation, A-type crystals formed (Hellman, Fairchild, & Senti, 1954; Karim et al., 2000). Conversely, the starch paste formed B-type crystals when the moisture content was higher than 43%. The relative crystallinity of ACS4 was 45.25%, while the lowest relative crystallinity was 37.96% (ACS-80). This might be because that when the temperature was below 0 °C, the lower the temperature was, the faster the cooling rate and the lower the relative crystallinity was. At a fast cooling rate, the migration of molecular chains was blocked, which affected the rearrangement of amylose and hindered the formation of perfect crystals. In a single storage temperature environment, the recrystallization process of B-type crystals was strongly restricted by nucleation, and the recrystallization degree of rice starch was highest near the optimum nucleation temperature. The optimum nucleation was

Table 4
Crystal cell parameters of ACS.

Samples	ACS-80	ACS-18	ACS4	ACS25
a (Å)	6.26 ± 0.00^{d}	6.72 ± 0.00^{c}	10.11 ± 0.07^{a}	9.43 ± 0.01^{b}
b (Å)	6.26 ± 0.00^{d}	6.72 ± 0.00^{c}	10.11 ± 0.07^{a}	9.43 ± 0.01^{b}
c (Å)	16.97 ± 0.00^{a}	16.79 ± 0.06^{a}	16.54 ± 0.33^{b}	15.29 ± 0.01^{c}
α (°)	90	90	90	90
β (°)	90	90	90	90
γ (°)	120	120	120	120
V (Å^3)	575.95 ± 0.00^{d}	656.63 ± 2.35^{c}	1464.41 ± 49.49^{a}	1177.50 ± 3.27^{b}
R (%)	6.16	7.72	7.53	7.18

ACS-80, amylose crystal seeds prepared by RA-80; ACS-18, amylose crystal seeds prepared by RA-18; ACS4, amylose crystal seeds prepared by RA4; and ACS25, amylose crystal seeds prepared by RA25; R, fitting error.
Values in the same line with different lowercase letters are significantly different ($p < 0.05$).

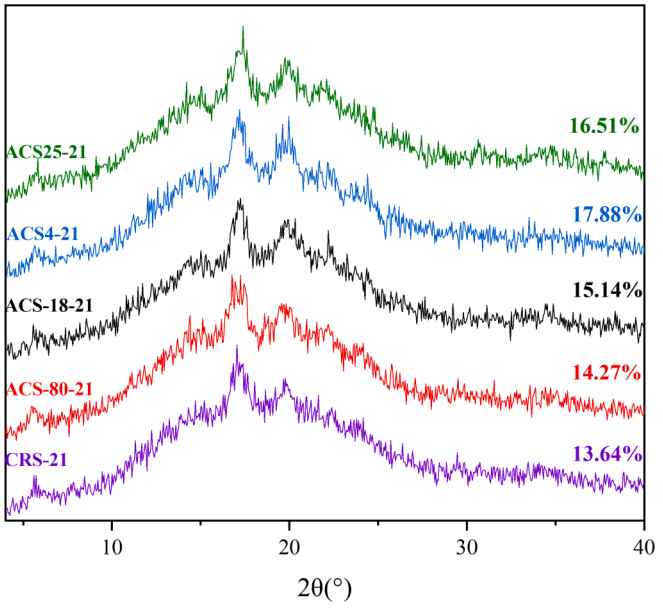

Fig. 2. X-ray diffraction patterns and relative crystallinity of 21 day retrograded starch (CRS-21, ACS-80-21, ACS-18-21, ACS4-21 and ACS25, respectively, from bottom to up; 2θ means the diffraction angle).

4 °C (Baik, Kim, Cheon, Ha, & Kim, 1997), so the degree of retrogradation was the highest at 4 °C. The formed crystal nucleus grown fastest at 30 °C and was possible to melt at temperature above 30 °C, so with the increase of storage temperature, the melting degree increased and the retrogradation degree decreased. In the early stage of cooling and nucleation of four groups of ACS, the nucleation degree of ACS4 was the best, while in the later stage of thermal insulation growth, the growth condition was limited by the nucleation in the early stage, so the recrystallization degree of ACS4 was the highest and the condition of recrystallization was the best.

The software Jade 6.5 was used to determine the crystal cell parameters of ACS. The results are shown in Table 4. R represents the fitting error. The smaller the R value, the better the fit. All four ACS had R values less than 9%, indicating that the fitting result was credible. According to previous results, all four ACS belonged to the hexagonal crystal system (Buléon, Véronèse, & Putaux, 2007; Imberty & Perez, 1988). Their crystal cell structure was slender and the lengths of their c axes exhibited little differences. However, the a and b axis lengths of ACS4 and ACS25 were significantly longer than those of ACS-80 and ACS-18. The crystal cell volume of ACS-80, ACS-18, ASC4, and ACS25 were 575.95, 656.63, 1464.41, and 1177.50 Å^3, respectively. Among the four types of ACS, ACS4 had the loosest crystal cell structure and largest crystal cell volume. On the contrary, ACS-80 had the tightest crystal cell structure and smallest crystal cell volume. The reason for this might be due to the fact that 4 °C was suitable for crystal nucleation, the starch migrated and rearranged rapidly, a large number of small particles and uneven crystal seeds were formed during this process and it formed loose starch structure finally. Furthermore, under the condition of fast cooling, the molecular thermal movement slowed down and the molecular migration was hindered, so the crystal cell structure of ACS-80 was the loosest.

Table 5
The R1 value and R2 value of retrograded starch.

Sample names	R1	R2
CRS-21	0.670 ± 0.005^{e}	1.246 ± 0.004^{a}
ACS-80-21	0.731 ± 0.003^{d}	1.220 ± 0.006^{b}
ACS-18-21	0.800 ± 0.002^{c}	1.149 ± 0.002^{c}
ACS4-21	0.887 ± 0.003^{a}	1.029 ± 0.003^{e}
ACS25-21	0.853 ± 0.012^{c}	1.043 ± 0.004^{d}

R1, the ratio of absorbance at 1047 to 1022 cm^{-1}; R2, the ratio of absorbance at 1022 to 995 cm^{-1}.
CRS-21, 21 day control retrograded starch; ACS-80-21, 21 day retrograded starch added with ACS-80; ACS-18-21, 21 day retrograded starch added with ACS-18; ACS4-21, 21 day retrograded starch added with ACS4; ACS25-21, 21 day retrograded starch added with ACS25.
Values in the same column with different lowercase letters are significantly different ($p < 0.05$).

3.2. Crystal structure of retrograded starch affected by ACS

3.2.1. Long-range order of retrograded starch

The XRD patterns and relative crystallinity of 21 day retrograded starch samples are shown in Fig. 2. This shows that the addition of ACS didn't alter the crystal type of retrograded starch, all of which retained B-type crystal structures. The relative crystallinity of the control retrograded starch was 13.64%, while the relative crystallinities of retrograded starch containing ACS-80, ACS-18, ACS4, and ACS25 were 14.27%, 15.14%, 17.88%, and 16.51%, respectively. The relative crystallinities of samples with ACS were all higher than that of the control, indicating that addition of ACS could enhance long-range order and promote long-term retrogradation. Additionally, samples with ACS showed a higher diffraction intensity peak at 17° than control retrograded starch. The 17° peak corresponded to the aggregation state of the amylose double helix (Chen et al., 2019), suggesting that addition of ACS promoted the aggregation of the amylose.

3.2.2. Short-range order of retrograded starch

Starch granules consist of a crystalline region and an amorphous region. Amylose and short chains of amylopectin form a double helix structure, which is referred to as a short-range ordered structure. These double helix chains form intermolecular interactions within the starch granules to form a long-range ordered structure, i.e., a crystal. Currently, FTIR and Raman spectroscopy are the main methods used to study the short-range ordered structure of starch. Here, FTIR was used to study the short-range ordered structure of 21 day retrograded starch. The absorption peak at 1047 cm^{-1} corresponded to the crystalline structure of starch aggregates, while the absorption peak at 1022 cm^{-1} corresponded to the irregular agglomeration of starch macromolecules, and the absorption peak at 995 cm^{-1} corresponded to the bending vibrations of hydroxyl groups on starch chains (Li, Pernell, & Ferruzzi, 2018; Sevenou, Hill, Farhat, & Mitchell, 2002). The ratio of absorbance at 1047 to 1022 cm^{-1} and the ratio of absorbance at 1022 to 995 cm^{-1} were used to characterize the degree of starch retrogradation, which were termed R1 and R2. The results are shown in Table 5. The value of R1 increased after adding ACS, while the value of R2 decreased after the addition of ACS. These results indicated that the addition of ACS improved the short-range order of long-term retrograded starch and increased the

Table 6
Crystal cell parameters of retrograded starch added with ACS.

Samples	CRS-21	ACS-80-21	ACS-18-21	ACS4-21	ACS25-21
a (Å)	6.46 ± 0.00^{e}	6.92 ± 0.00^{d}	9.53 ± 0.01^{c}	17.72 ± 0.03^{a}	10.31 ± 0.07^{b}
b (Å)	6.46 ± 0.00^{e}	6.92 ± 0.00^{d}	9.53 ± 0.01^{c}	17.72 ± 0.03^{a}	10.31 ± 0.07^{b}
c (Å)	16.77 ± 0.00^{a}	16.79 ± 0.06^{ab}	15.29 ± 0.01^{d}	16.32 ± 0.03^{c}	16.54 ± 0.33^{bc}
α (°)	90	90	90	90	90
β (°)	90	90	90	90	90
γ (°)	120	120	120	120	120
V (Å)^{3}	699.84 ± 0.00^{e}	803.53 ± 3.35^{d}	1389.57 ± 4.74^{c}	4437.93 ± 23.18^{a}	1754.93 ± 55.19^{b}
R (%)	6.13	6.16	7.72	7.53	7.18

CRS-21, 21 day control retrograded starch; ACS-80-21, 21 day retrograded starch added with ACS-80; ACS-18-21, 21 day retrograded starch added with ACS-18; ACS4-21, 21 day retrograded starch added with ACS4; ACS25-21, 21 day retrograded starch added with ACS25; R, fitting error.
Values in the same line with different lowercase letters are significantly different ($p < 0.05$).

Table 7
Avrami index and rate constant of retrograded starch at 4 °C.

Samples	Retrogradation rate constant (d^{-1})	Avrami index	R^2
CRS-21	0.024 ± 0.003^{d}	1.869 ± 0.023^{a}	0.967
ACS-80-21	0.034 ± 0.002^{c}	1.613 ± 0.009^{c}	0.978
ACS-18-21	0.036 ± 0.002^{c}	1.667 ± 0.012^{b}	0.964
ACS4-21	0.051 ± 0.003^{a}	1.480 ± 0.010^{d}	0.978
ACS25-21	0.044 ± 0.002^{b}	1.689 ± 0.020^{b}	0.935

CRS-21, 21 day control retrograded starch; ACS-80-21, 21 day retrograded starch added with ACS-80; ACS-18-21, 21 day retrograded starch added with ACS-18; ACS4-21, 21 day retrograded starch added with ACS4; ACS25-21, 21 day retrograded starch added with ACS25.
Values in the same column with different lowercase letters are significantly different ($p < 0.05$).

content of double helix during long-term retrogradation.

3.2.3. Crystal cell parameters of retrograded starch

Crystal cell parameters of retrograded starch were analyzed and the results are summarized in Table 6. The R values of all samples were less than 9%, indicating that the fitting result was credible. In this study, both ACS and retrograded starch formed B-type crystal structures. The addition of ACS had no effect on the crystal system of the retrograded starch but altered their crystal cell parameters. Compared with control retrograded starch, the a and b axes lengths of retrograded starch in the experimental group all increased, while the c axis was slightly shorter. The rice starch added with ACS had a looser crystal cell structure and a larger crystal cell volume. These changes are potentially related to the effect of the crystal nucleus on crystal growth. After nucleation, the molecular chains aggregate towards the crystal nucleus and arrange in an ordered manner enabling the crystal grain to grow. The irregularly entangled molecular chains need to be unwound before they enter the crystalline region, as their irregularity prevents them from directly forming an ordered structure. However, in many cases, the molecular chains are often too late to be fully unwound and instead are arranged according to the adjacent crystal nucleus and enter the lattice to enable crystal grow. Therefore, the crystal cell structure of a crystal growing on the surface of a crystal nucleus is affected by the crystal cell structure of the crystal nucleus, which will determine the crystal cell parameters of subsequent crystals.

3.3. Nucleation pattern of retrograded starch with ACS

The kinetics of retrogradation was studied using DSC. The results were fitted using equation (3) to obtain the retrogradation kinetic parameters which are shown in Table 7.

Table 7 shows that the Avrami index (n) decreased after the addition of ACS. According to previous studies, rice starch gels show an instantaneous nucleation pattern during nucleation when $n < 1$, while they show a continuous nucleation pattern in nucleation process when $n > 1$ (Tian et al., 2009; Lian, Zhao, Liu, & Zhang, 2011).

According to Shi et al. (2016), high n values are related to a lower retrogradation rate. In this study, native rice starch and starch added with ACS both formed continuous nucleation patterns during the nucleation process. The n values of the experimental groups were smaller than the control, indicating that the addition of ACS accelerated nucleation. Among them, the nucleation rate of retrograded starch containing ACS4 was the fastest, which may be due to the fact that ACS4 has the highest relative crystallinity and degree of short-range order. In addition, the rate constant of retrogradation increased after the addition of ACS, strongly indicating that ACS promotes retrogradation.

4. Conclusions

ACS could enter the gelatinized starch and induct the long-term retrogradation of starch. It increased the relative crystallinity of retrograded starch and improved the long-range and short-range ordered degree of long-term retrograded starch. The crystal cell of retrograded starch was looser and had a larger volume in the presence of ACS. In addition, ACS promoted nucleation and retrogradation during long-term retrogradation. Overall, these results suggest that ACS increased long-term retrogradation and it could be used to prepare starch with slow digestibility in future.

Declaration of competing interest

The authors declare that they have no known competing financial interests or personal relationships that could have appeared to influence the work reported in this paper.

Acknowledgments

This study was financially supported by the National Natural Science Foundation of China (Nos. 31972027 and 31901731) and the Ten Thousand Talent Program Youth Top-notch Talent Project of China.

References

Angellier, H., Choisnard, L., Molina-Boisseau, S., Ozil, P., & Dufresne, A. (2004). Optimization of the preparation of aqueous suspensions of waxy maize starch nanocrystals using a response surface methodology. *Biomacromolecules, 5*(4), 1545–1551.
Avrami, M. (1939). Kinetics of phase change. I General theory. *The Journal of Chemical Physics, 7*(12), 1103–1112.
Baik, M. Y., Kim, K. J., Cheon, K. C., Ha, Y. C., & Kim, W. S. (1997). Recrystallization kinetics and glass transition of rice starch gel system. *Journal of Agricultural and Food Chemistry, 45*(11), 4242–4248.
BeMiller, J. N., & Whistler, R. L. (2008). *Starch chemistry and technology* (3rd ed.). Netherlands: Elsevier (Chapter 13).
Buléon, A., Véronèse, G., & Putaux, J. L. (2007). Self-association and crystallization of amylose. *Australian Journal of Chemistry, 60*(10), 706–718.
Bulkin, B. J., Kwak, Y., & Dea, I. C. M. (1987). Retrogradation kinetics of waxy-corn and potato starches; a rapid, Raman-spectroscopic study. *Carbohydrate Research, 160*(87), 95–112.
Cheng, K., Xu, Y., Xiong, S., & Zhao, S. (2008). Separating and purifying rice amylose by recrystallization. *Journal of the Chinese Cereals and Oils Assocciation, 23*(2), 170–173.
Chen, L., Ren, F., Zhang, Z., Tong, Q., & Rashed, M. (2015). Effect of pullulan on the short-term and long-term retrogradation of rice starch. *Carbohydrate Polymers, 115*, 415–421.
Chen, L., Tian, Y., McClements, D. J., Huang, M., Zhu, B., Wang, L., et al. (2019). A simple and green method for preparation of non-crystalline granular starch through controlled gelatinization. *Food Chemistry, 274*, 268–273.
Chen, L., Tian, Y., Sun, B., Cai, C., Ma, R., & Jin, Z. (2018). Measurement and characterization of external oil in the fried waxy maize starch granules using ATR-FTIR and XRD. *Food Chemistry, 242*, 131–138.

Funami, T. (2009). Functions of food polysaccharides to control the gelatinization and retrogradation behaviors of starch in an aqueous system in relation to the macromolecular characteristics of food polysaccharides. *Food Science and Technology Research, 15*(6), 557–568.

Fu, Z. Q., Wang, L. J., Li, D., Zhou, Y. G., & Adhikari, B. (2013). The effect of partial gelatinization of corn starch on its retrogradation. *Carbohydrate Polymers, 97*(2), 512–517.

Hellman, N., Fairchild, B., & Senti, F. (1954). The bread staling problem-molecular organization of starch upon aging of concentrated starch gels at various moisture levels. *Cereal Chemistry, 31*(6), 495–505.

Imberty, A., Bulecon, A., Tran, V., & Péerze, S. (1991). Recent advances in knowledge of starch structure. *Starch/Stärke, 43*, 375–384.

Imberty, A., & Perez, S. (1988). A revisit to the three-dimensional structure of B-type starch. *Biopolymers: Original Research on Biomolecules, 27*(8), 1205–1221.

Karim, A. A., Norziah, M. H., & Seow, C. C. (2000). Methods for the study of starch retrogradation. *Food Chemistry, 71*(1), 9–36.

Kim, J., Kim, W., & Shin, M. (1997). A comparative of rice starch and α-amylase study on retrogradation gels by DSC, X-ray methods. *Starch/Stärke, 49*(2), 71–75.

Lian, X., Liu, L., Guo, J., Li, L., & Wu, C. (2013). Screening of seeds prepared from retrograded potato starch to increase retrogradation rate of maize starch. *International Journal of Biological Macromolecules, 60*, 181–185.

Lian, X., Zhao, S., Liu, Q., & Zhang, X. (2011). A photographic approach to the possible mechanism of retrogradation of sweet potato starch. *International Journal of Biological Macromolecules, 48*(1), 125–128.

Li, M., Pernell, C., & Ferruzzi, M. G. (2018). Complexation with phenolic acids affect rheological properties and digestibility of potato starch and maize amylopectin. *Food Hydrocolloids, 77*, 843–852.

Marentette, J. M., & Brown, G. R. (1993). Polymer spherulites: II. Crystallization kinetics. *Journal of Chemical Education, 70*(7), 539.

Mciver, R. G., Axford, D. W. E., Colwell, K. H., & Elton, G. A. H. (1968). Kinetic study of the retrogradation of gelatinised starch. *Journal of the Science of Food and Agriculture, 19*(10), 560–563.

Ronda, F., & Roos, Y. H. (2008). Gelatinization and freeze-concentration effects on recrystallization in corn and potato starch gels. *Carbohydrate Research, 343*(5), 903–911.

Sevenou, O., Hill, S. E., Farhat, I. A., & Mitchell, J. R. (2002). Organisation of the external region of the starch granule as determined by infrared spectroscopy. *International Journal of Biological Macromolecules, 31*(1–3), 79–85.

Shi, M., & Gao, Q. (2016). Recrystallization and in vitro digestibility of wrinkled pea starch gel by temperature cycling. *Food Hydrocolloids, 61*, 712–719.

Swinkels, J. J. M. (1985). Composition and properties of commercial native starches. *Starch/Stärke, 37*(1), 1–5.

Tian, Y., Li, Y., Manthey, F. A., Xu, X., Jin, Z., & Deng, L. (2009). Influence of β-cyclodextrin on the short-term retrogradation of rice starch. *Food Chemistry, 116*(1), 54–58.

Tukomane, T., & Varavinit, S. (2008). Classification of rice starch amylose content from rheological changes of starch paste after cold recrystallization. *Starch/Stärke, 60*, 292–297.

Yao, Y., Zhang, J., & Ding, X. (2002). Structure-retrogradation relationship of rice starch in purified starches and cooked rice grains: A statistical investigation. *Journal of Agricultural and Food Chemistry, 50*(25), 7420–7425.